Physics and Chemistry of the Earth 85–86 (2015) 201–209

Contents lists available at ScienceDirect

Physics and Chemistry of the Earth

journal homepage: www.elsevier.com/locate/pce

Multiresolution wavelets and natural time analysis before the January–February 2014 Cephalonia (Mw6.1 & 6.0) sequence of strong earthquake events

Filippos Vallianatos [a,b,*], Georgios Michas [b], George Hloupis [c]

[a] Technological Educational Institute of Crete, Laboratory of Geophysics and Seismology, Chania 73100, Crete, Greece
[b] Institute for Risk and Disaster Reduction, University College London, Gower Str., London WC1E 6BT, UK
[c] Technological Educational Institute of Athens, Egaleo, 12210 Athens, Greece

A R T I C L E I N F O

Article history:
Received 22 January 2015
Received in revised form 27 May 2015
Accepted 15 June 2015
Available online 30 July 2015

Keywords:
Multiresolution wavelets
Natural time analysis
Cephalonia
Seismicity

A B S T R A C T

On January 26 and February 3, 2014, Cephalonia Island (Ionian Sea, Greece) was struck by two strong, shallow earthquakes (moment magnitudes Mw6.1 and Mw6.0, respectively) that ruptured two sub-parallel, strike-slip faults, with right-lateral kinematics. The scope of the present work is to investigate the complex correlations of the earthquake activity that preceded the Mw6.1 event in the broader area of the Cephalonia Island and identify possible indications of critical stages in the evolution of the earthquake generation process. We apply the recently introduced methods of Multiresolution Wavelet Analysis (MRWA) and Natural Time (NT) analysis and for the first time we combine their results in a joint approach that may lead to universal principles in describing the evolution of the earthquake activity as it approaches a major event. In particular, the initial application of MRWA on the inter-event time series indicates a time marker 12 days prior to the major event. By using this time as the initiation point of the NT analysis, the critical stage of seismicity, where the κ_1 parameter reaches the critical value of $\kappa_1 = 0.070$, is approached few days before the occurrence of the Mw6.1 earthquake.

1. Introduction

On January 26, 2014 an Mw6.1 earthquake occurred in the western part of the Cephalonia Island that is one of the most seismically active regions in the Eastern Mediterranean region. In modern times, the most prominent earthquakes in the area were those that ruptured the Eastern part of the island on 9, 11 and 12 August, 1953, with surface-wave magnitudes of 6.4, 6.8 and 7.2, respectively (Papazachos and Papazachou, 1997). On 17 January, 1983 a large (Mw7.0) earthquake ruptured the western offshore part with no significant damages (see Kiratzi and Langston, 1991; Tzanis et al., 2000 and references therein). The current seismic excitation is the result of right lateral shear strain accumulated on a zone of weakness, which abuts and slightly overlaps the rupture area of the 1983 main shock (Mw7.0) (Papadimitriou, 2002; Karakostas et al., 2014).

In the last several years, strong evidence indicates that earthquake generation process can be viewed as a critical phenomenon, culminating with a large event that corresponds to some critical point (Bak and Tang, 1989; Rundle et al., 2003; Sornette, 2000; Kiyashchenko et al., 2003, 2004; Uritsky et al., 2004; Zoeller and Hainzl, 2002 and references therein). In addition, it has recently been shown that a wide variety of geodynamic phenomena related to the complexity dynamics reveals features that could be interpreted in the framework of new views as that of non-extensive statistical physics (Tsallis, 2009), the multiresolution wavelets analysis (Telesca et al., 2004, 2007) and of the newly defined time domain, termed natural time approach (Varotsos et al., 2002, 2006, 2011a; Sarlis et al., 2010).

Time dynamics characterization of an earthquake sequence gives strong evidence for the existence of an underlying spatiotemporal nonlinear deterministic dynamical process (Telesca et al., 2000, 2001, 2002, 2004). The observed time–space behaviour can be mapped by fractal (self-similar) properties such as power laws profiles, long range correlations and space–time clustering (Lapenna et al., 2000; Telesca et al., 2002; Telesca and Macchiato, 2004; Papadakis et al., 2013; Antonopoulos et al., 2014) and can describe the spatial and temporal distribution of earthquakes (see Davidsen and Goltz, 2004; Abe and Suzuki, 2005; Corral and Christensen, 2006; Michas et al., 2013).

* Corresponding author at: Technological Educational Institute of Crete, Laboratory of Geophysics and Seismology, Chania 73100, Crete, Greece.
E-mail address: fvallian@chania.teicrete.gr (F. Vallianatos).

http://dx.doi.org/10.1016/j.pce.2015.06.001
1474-7065/

Recently and in order to analyse Seismic Electric Signals (SES), the concept of natural time was introduced (see Varotsos et al., 2011a and references therein). Varotsos et al., show that an interrelation exists between the time evolution of the seismic activity measured from the start of the SES and the spectrum characteristics of the SES in natural time (Varotsos et al., 2002, 2009, 2011a and references therein). Furthermore, the analysis of complex systems using the natural time approach, as has been shown in Abe et al. (2005), reduces the uncertainties, allowing the optimal extraction of signal information and enables (Varotsos et al., 2011a, 2011b and references therein) the identification of long-range correlations even in the presence of "heavy tails". The consistency of natural time analysis in approaching the complex dynamics of critical phenomena, such as seismicity, fracturing, 2-D Ising model, 3-D turbulent flow and acoustic emissions experiments, has been demonstrated in a series of recent studies (Varotsos et al., 2002, 2005a, 2005b; Vallianatos et al., 2013, 2014 and references therein).

In addition, wavelet-based methods have been proved quite useful in the characterization of fractal signals (Thurner et al., 1997; Abry et al., 2000, 2002). Wavelet analysis also enjoys the salutary property that is not vulnerable to non-stationarities (Wornell, 1995; Teich et al., 1996; Abry and Veitch, 1998); a situation that is not very rare when characterizing the time dynamics of an earthquake sequence.

Our research is motivated by the history of large earthquakes in the Cephalonia Transform Fault (see Papazachos and Papazachou, 1997) and the need of testing and evaluating the predictive capability of the natural time analysis in an area that has been shown to generate precursory effects (Tzanis et al., 2000).

The scope of the present work is twofold. We investigate the applicability of natural time analysis (NT) (Varotsos et al., 2011a) in the seismicity prior to the Cephalonia Mw6.1 strong earthquake, introducing the results of multiresolution wavelets analysis (MRWA) on the interevent time sequences, in order to define one of the crucial parameters, which is the starting point in the NT. The question of whether seismicity is described by Natural Time parameters, as modified by introducing the results of MRWA as the initiation point for the NT, even at the phenomenological level, represents a challenge, possibly leading to universal principles in describing the evolution of the earthquake generation processes.

2. The Tectonic setting and seismicity of Cephalonia region

The Ionian Islands in the Western Greece lay on a seismotectonically complex area that is undergoing rapid and intense ground deformation. The Cephalonia Island, in the central l part of Ionian region (Fig. 1), has a remarkable seismic history which can be traced back to antiquity (Papazachos and Papazachou, 1997). The island was formed during Tertiary as a result of the convergence between the African and the Eurasian plates that initiated at the end of the Cretaceous (Kokinou et al., 2006 and references therein). It mainly consists of Alpine Mesozoic and Cenozoic sedimentary rocks belonging to the External Hellenides, the Paxos or Pre-Apulian zone and the overthrusted Ionian zone (Lekkas et al., 2001). Cephalonia has been repeatedly subjected to strong ground shaking due to the proximity of the island to the Cephalonia Transform Fault (CTF) (Fig. 1). CTF (Scordilis et al., 1985) lies offshore to the west of the Cephalonia Island and is a major strike-slip fault that links the subduction boundary to the continental collision between the Apulian microplate and the Hellenic foreland (Sachpazi et al., 2000) and plays a key role in the region's geodynamic complexity (LePichon et al., 2002; Louvari et al., 1999) (see Fig. 1). Its slip-rate varies from 7 to 30 mm/yr (Hollenstein et al., 2008), which is consistent with seismological data (Papazachos and Kiratzi, 1996).

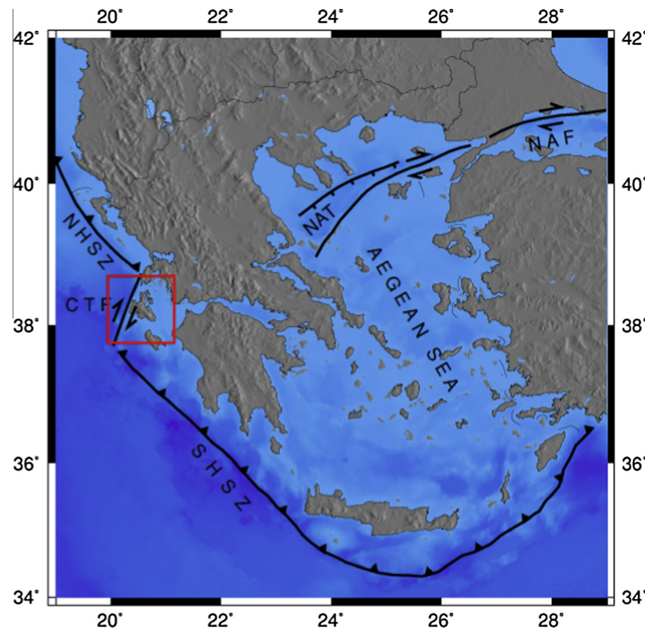

Fig. 1. Key seismotectonic features of the broader Aegean area. SHSZ is the South Hellenic Subduction Zone, NHSZ the North Hellenic Subduction Zone, CTF the Cephalonia Transform Fault, NAT the North Aegean Trough and NAF the North Anatolian Fault. The rectangle marks the study area.

For this region, complete historical information exists for strong ($M \geqslant 6.5$) earthquakes in the last five centuries, revealing an average of about one such shock per decade (Papadimitriou and Papazachos, 1985). The most severe was the 1953 paroxysm with four events (9 August, M 6.4; 11 August, M 6.8; 12 August, M 7.2; 21 October, M 6.3) that almost completely destroyed the infrastructures on the Cephalonia Island. The most recent large CTF events include the M6.8, January 17, 1983 and the M6.2, August, 14, 2003. Two strong earthquake events, with Mw6.1 and Mw6.0, occurred on January 26, 2014 (13:55 UTC) and February 3, 2014 (03:08 UTC) respectively, onshore the island of Cephalonia (Ganas et al., 2014; Karastathis et al., 2014), inducing extensive structural damages and environmental effects, mainly in the western and central parts (Valkaniotis et al., 2014 and references therein).

Recent upgrading of the seismological networks operating in the area (Mignan and Chouliaras, 2014) permits the use of an accurate catalogue to analyse the microseismicity of the area. The seismicity data used in this study are taken from the Hellenic Unified Seismological Network (HUSN) (Mignan and Chouliaras, 2014; D'Alessandro et al., 2011; Papanastassiou, 2010), the development of which took place gradually from the end of 2007 to 2011. The dataset is available from the catalogue of the Geodynamic Institute of the National Observatory of Athens (GI-NOA, http://www.gein.noa.gr). As reported in Mignan and Chouliaras (2014), the 2011 upgrading of the HUSN has resulted in the significant improvement of the network's performance. In Mignan and Chouliaras (2014), the Bayesian Magnitude of Completeness (BMC) method has been used to provide a complete spatial coverage of the magnitude of completeness (Mc) for the area of Greece, demonstrating that the value of Mc in the area of Cephalonia is down to 2.0. In addition, it was indicated that the application of the routinely used test that is based on the Gutenberg–Richter scaling relation, yields biased results on the completeness magnitude, depending on the level of complexity of the data set considered. Fig. 2 presents the observed seismicity in the Cephalonia region during a period starting 150 days before the January 26, 2014 event in an area of radius R = 50 km around the major event. The solid black line marks the Cephalonia Transform Fault (CTF).

3. Multiresolution wavelets analysis in the seismicity of Cephalonia region

The study of temporal distribution of seismic events is a crucial subject when dealing with their time-scaling properties (Godano and Caruso, 1995; Telesca et al., 2002; Öncel et al., 1996; Hainzl et al., 2006) since it contributes to the understanding of the correlation properties of seismicity along with its scaling properties (Corral and Christensen, 2006). The analysis of time intervals between successive seismic events can be grouped in exponential or power laws revealing similar behaviours in different scales (Abe and Suzuki, 2005).

A Wavelet Transform (WT) involves the decomposition of a signal function or vector into simpler, fixed building blocks at different scales and positions. In a similar way as Fourier transform (FT) does, WT operates on a signal and transforms it from time domain to Wavelet domain. In Fourier analysis, only the sine and cosine functions (which are localized in frequency domain) can be applied to a function, with a difficulty to process a function having components that are localized in the time domain. As a result, a small frequency change in FT produces changes everywhere in this domain. On the other hand, wavelet functions are localized both in frequency or scale and in time via dilations and translations of the mother wavelet, respectively. This leads to compact representation of large classes of functions and operators in the Wavelet domain. This is one of the major advantages of WT: an event can be simultaneously described in the frequency domain as well as in the time domain, unlike the usual Fourier transform where an event is accurately described either in the frequency or in the time domain. As a consequence, MRWA of data with different behaviour on different scales can be highly benefited by use of WT.

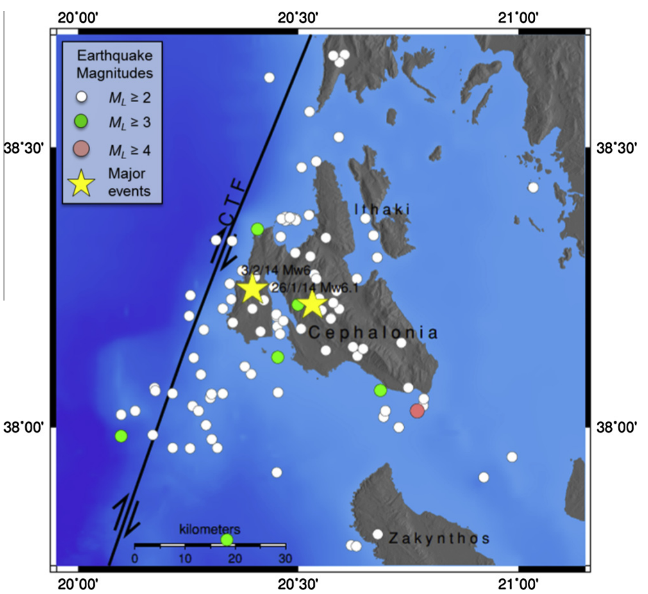

Fig. 2. The observed seismicity in the Cephalonia region during a period starting 150 days before the January 26, 2014 event in an area of radius $R = 50$ km around the major event. The solid black line marks the Cephalonia Transform Fault (CTF).

The discrete wavelet transform (DWT) transforms a data vector of length M into a different vector of the same length. The DWT can be considered as a filtering technique under the terminology of signal processing. A wavelet basis is characterized by a particular set of numbers called wavelet filter coefficients. In practice, DWT is commonly implemented using dyadic multirate filter banks (consisting of high and low pass filters) which divide the signal frequency band into sub bands. At each scale, detail coefficients are generated from the output of high-pass filters, since approximation coefficients are outputs from low-pass filters. For a point process such as the interevent times sequence, the wavelet coefficients can be derived from:

$$W_{m,n}^{wav} = 2^{-m/2}\sum_{i=1}^{L} t_i \psi(2^{-m}i - n) \tag{1}$$

where the scale variable m and the translation variable n are integers, L represents the total number of interevent times t_i and ψ is the wavelet function. The DWT is evaluated at the points (m, n) in the scale-interval-number plane. Smaller scales correspond to more rapid variations and therefore to higher frequencies.

In the current study we perform MRWA by examining the standard deviation of wavelet coefficients as a function of scale as described from:

$$\sigma_{wav}(m) = \sqrt{\frac{1}{N-1}\sum_{n=1}^{N}\left(W_{m,n}^{wav} - \langle W_{m,n}^{wav}\rangle\right)^2} \tag{2}$$

where N is the number of wavelet coefficients at a given scale m and the brackets indicate the average among the coefficients at a scale m. Fig. 3 presents the interevent times between two successive

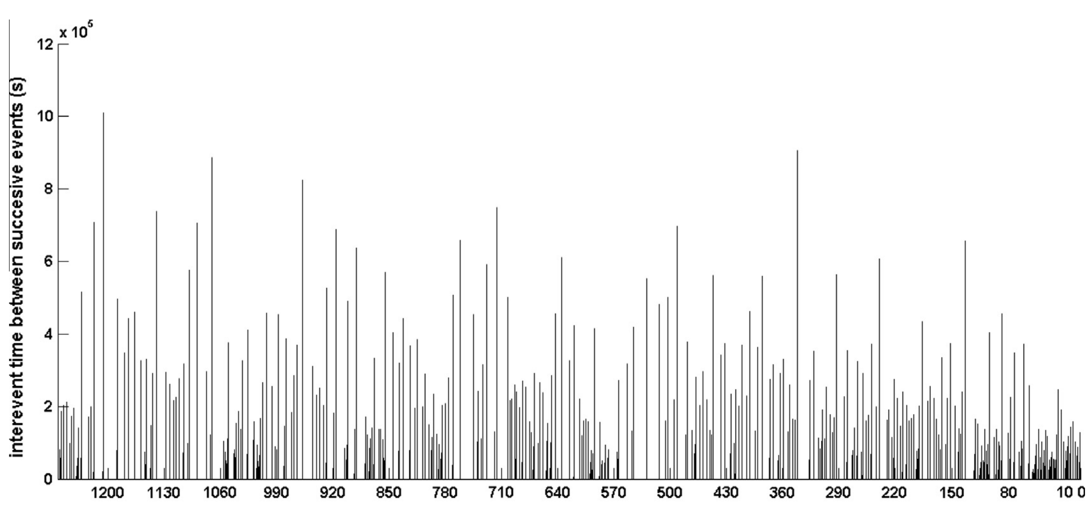

Fig. 3. Interevent times between two successive events versus time in days before the major event for a radius $R = 50$ km around epicenter and a magnitude threshold, $M_{th} = 2.0$.

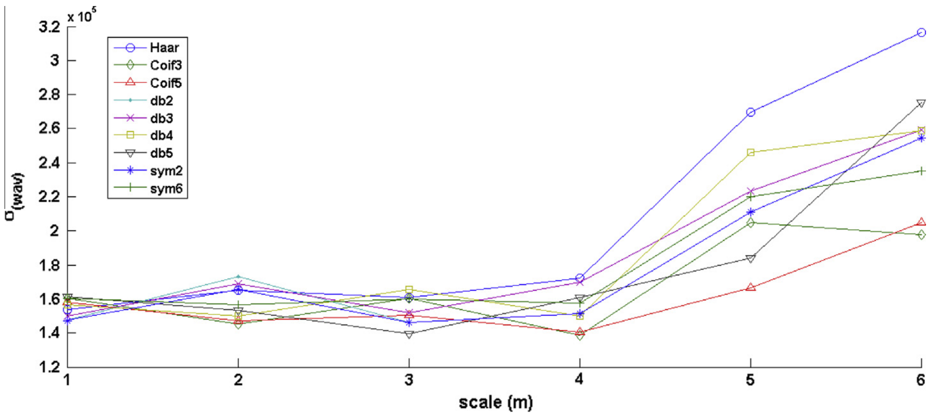

Fig. 4. $\sigma_{wav}(m)$ for the seismic catalogue (from 1/9/2010 until 26/1/2014) as calculated by means of different wavelet functions.

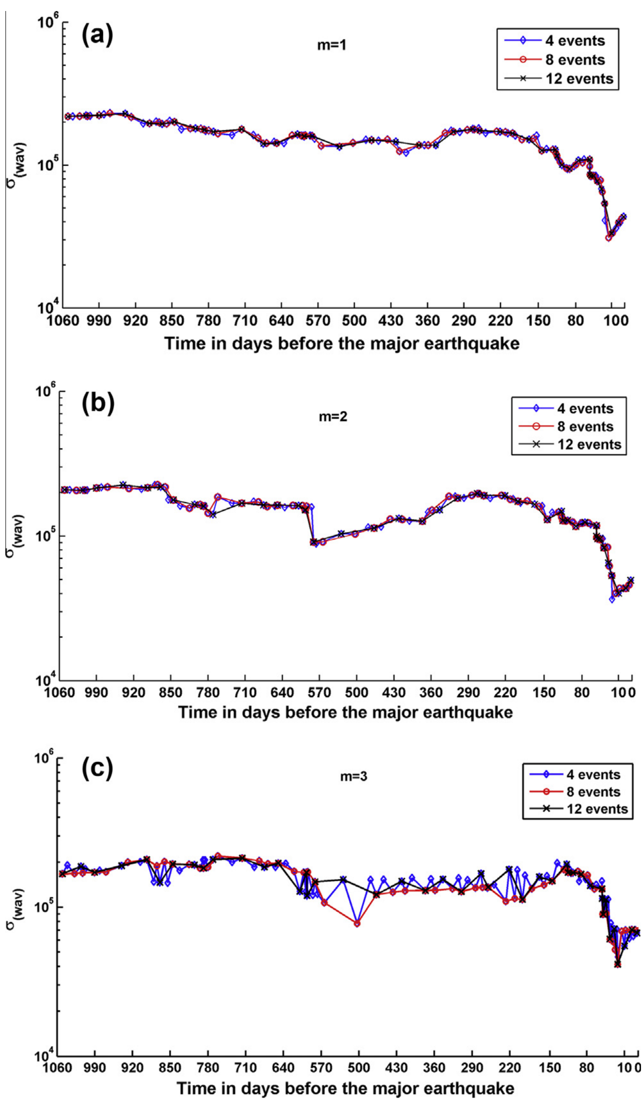

Fig. 5. Time variation of $\sigma_{wav}(m)$ with m ranging from 1 (a), 2(b) and 3(c), for moving window with 80 events and different shifts (4, 8 and 12 events as expressed in legend). Interevent times were estimated using the HUSN catalogue (from 1/9/2010 until 26/1/2014) with events within a radius $R = 50$ km around the M6.1 epicenter and a magnitude threshold, $M_{th} = 2.0$.

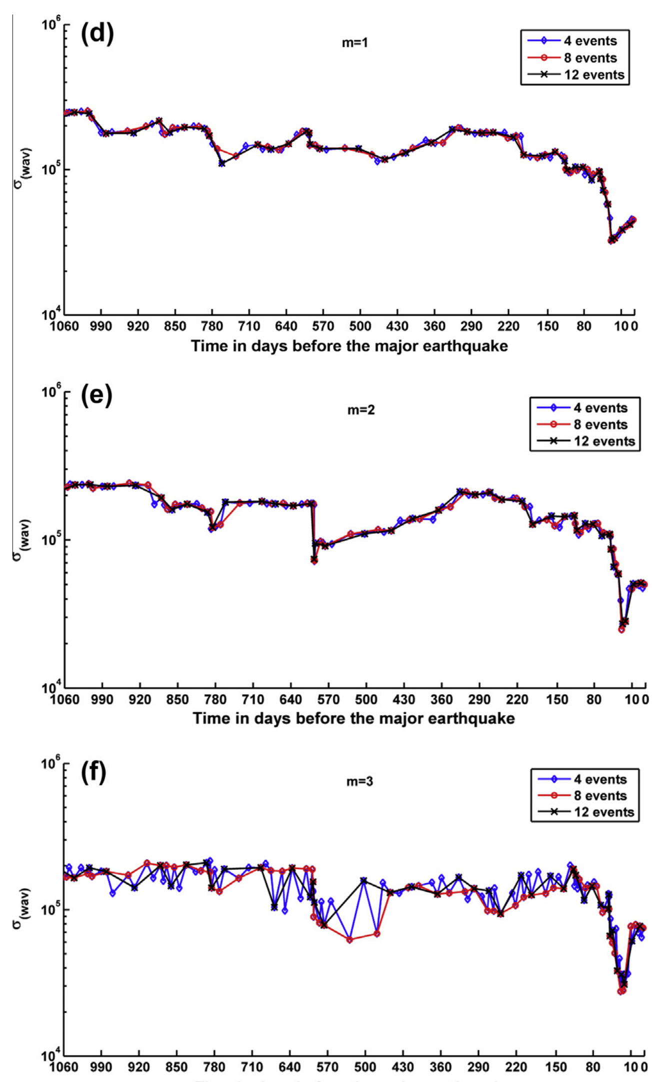

Fig. 6. Time variation of $\sigma_{wav}(m)$ with m ranging from 1 (d), 2(e) and 3(f), for moving window with 60 events and different shifts (4, 8 and 12 events as expressed in legend). Interevent times were estimated using the HUSN catalogue (from 1/9/2010 until 26/1/2014) with events within a radius $R = 50$ km around the M6.1 epicenter and a magnitude threshold, $M_{th} = 2.0$.

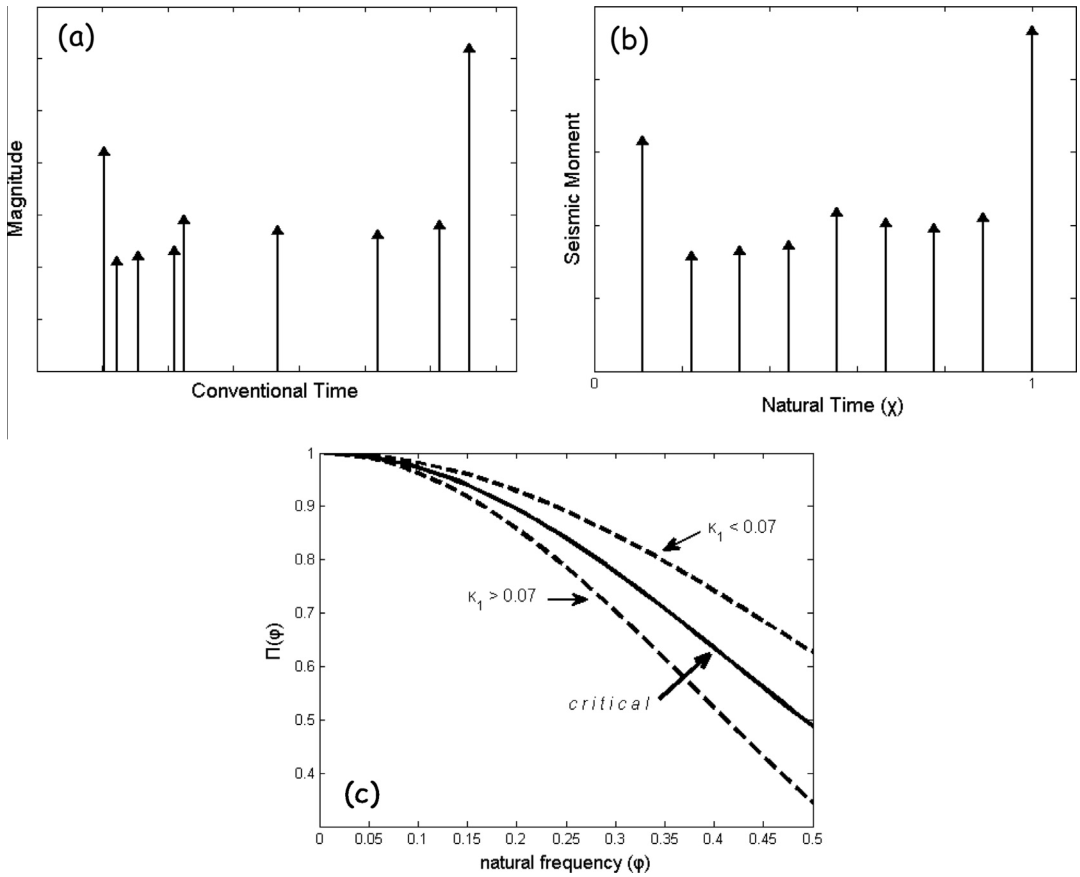

Fig. 7. Time series of seismic events (a) in conventional time t and (b) in the natural time χ. (c) Schematic diagram showing the power spectrum $\Pi(\phi)$ in natural time. Solid line is $\Pi(\phi)$ obtained from Eq. (4) for critical stage ($\kappa_1 = 0.070$), whereas two other lines are for $\kappa_1 > 0.07$ and $\kappa_1 < 0.07$.

events versus the time occurrence of the second event until the major seismic event in a region within a circle of radius $R = 50$ km around epicenter and a magnitude threshold, $M_{\text{th}} = 2.0$. The time period that covered for MRWA of interevent times spans from 1/9/2010 until 26/1/2014.

A challenging question regarding WT involves the suitability of the analysing wavelet. In order to overcome the uncertainty of appropriate wavelet selection, initially, we perform calculation of the standard deviation of the wavelet coefficients $\sigma_{wav}(m)$, using different wavelets. Results are shown in Fig. 4 where the important observation is the significant variability of the wavelet coefficients, suggested by the high value of $\sigma_{wav}(m)$ as the scale increases; this is an indication of the strong fluctuations displayed by the original series. The increase of $\sigma_{wav}(m)$ with the scale indicates that the fluctuations of higher frequency are less strong than those of lower frequency (since the lower scales are associated with higher frequency oscillations). All the wavelets furnish very close results at small scales up to $m = 4$. After that (since the number of the wavelet coefficients at high scales m becomes lower) a spreading effect among the standard deviations of different wavelets is evident.

We investigated the time evolution of the $\sigma_{wav}(m)$, using fixed event number windows (80 and 60 events) shifting through the entire series. Consistently with the length of the time window, we analysed the time variation of the $\sigma_{wav}(m)$ for lower scales ($m = 1$–3) since the number of available events is limited ($L = 610$). The shift between successive windows was set in 3 different values (4, 8 and 12 events) permitting sufficient smoothing among the values of the measures without losing the ability to derive sharp transitions. Each calculated value is associated with the time of the last event in the window. Different wavelets have been used giving almost similar results. Figs. 5 and 6 show are presentative set of results for the time evolution of the $\sigma_{wav}(m)$ using db2 wavelet with 3 scales for MRWA and for different window lengths as well as for different shifts.

At each subplot (a, b and c for moving window with 80 events; d, e and f for moving window with 80 events) results for corresponding scale ($m = 1$, 2 and 3) using different window shifting (4, 8 and 12 events) are presented. An initial comment from Figs. 5 and 6 is the significant temporal variability in the strength of the multiscale properties of the interevent times. As observed in previous studies (Telesca et al., 2004, 2007) before the major event of the seismic sequence a traceable decrease of the temporal evolution of the $\sigma_{\text{wav},m}(t)$ appeared, especially at lower scales. A data mining approach to the plots at Fig. 5 as well as at Fig. 6 dictates the search of a time marker beginning several days before the major event. The sharp decrease at lower scales ($m = 1$ and $m = 2$) which is observed around 12 days before the major event can be qualified for such a time marker since the decrease is evident for several days and is not altered significantly when we use different moving window lengths as well as different window shifts. This is quite adequate for ensuring that this decrease is not of uniform (random) type. Regarding the higher scales ($m = 3$), the sharp decrease associated with the largest event seems less pronounced in the case of smaller window length and it is mainly evidenced a more regular and cyclical structure, corresponding to lower frequency fluctuations of the series.

The results from the analysis of lower scales suggest the use of noticeable time marker which observed almost 12 days before major event as the initiation point for the Natural Time analysis that will follow. More specific, the initial application of MRWA in a broader time period reveals time segment where the NT analysis is going to investigate for indicators suggesting the entrance to critical stage.

4. Natural time analysis of seismicity before the Cephalonia Mw6.1, January 26, 2014 earthquake

The natural time analysis of a complex system has been presented in detail in Varotsos et al. (2011a). Here we recapitulate the concept of natural time analysis as applied in the seismicity of the Cephalonia region. In a time series consisting of N earthquakes, the *natural time* χ serves as an index for the occurrence of the kth event and is defined as $\chi_k = k/N$. For the analysis of seismicity the pair (χ_k, M_k) is considered, where M_k is the seismic moment released during the kth event (see Fig. 7). Considering the evolution of (χ_k, M_k), the continuous function $F(\omega)$ is defined as:

$$F(\omega) = \sum_{k=1}^{N} M_k \exp\left(i\omega \frac{k}{N}\right) \tag{3}$$

where $\omega = 2\pi\phi$ and ϕ stands for the *natural frequency*.

We normalize $F(\omega)$ dividing it by $F(0)$,

$$\Phi(\omega) = \frac{\sum_{k=1}^{N} M_k \exp\left(i\omega \frac{k}{N}\right)}{\sum_{n=1}^{N} M_n} = \sum_{k=1}^{N} p_k \exp\left(i\omega \frac{k}{N}\right), \tag{4}$$

where $p_k = M_k \Big/ \sum_{n=1}^{N} M_n$. The quantities p_k describe the probability to observe the earthquake event at *natural time* χ_k. Using Eq. (4) a normalized power spectrum can be obtained: $\Pi(\omega) = |\Phi(\omega)|^2$. It has been proved that for natural frequencies ϕ less than 0.5, $\Pi(\omega)$ or $\Phi(\omega)$ reduces to a characteristic function for the probability distribution p_k in the context of probability theory (Varotsos et al., 2002, 2011b) and thus the following relation holds:

$$\Pi(\omega) = \frac{18}{5\omega^2} - \frac{6\cos\omega}{5\omega^2} - \frac{12\sin\omega}{5\omega^3} \tag{5}$$

According to probability theory, the moments of a distribution and hence the distribution itself can be approximately determined, once the behaviour of the characteristic function of the distribution is known around zero. For $\omega \to 0$, Eq. (5) leads to:

$$\Pi(\omega) \approx 1 - \kappa_1 \omega^2, \tag{6}$$

where κ_1 is the variance in natural time, given as

$$\kappa_1 = \langle \chi^2 \rangle - \langle \chi^2 \rangle = \sum_{k=1}^{N} p_k \chi_k^2 - \left(\sum_{k=1}^{N} p_k \chi_k \right)^2 \tag{7}$$

It has actually been shown that the properties of $\Pi(\omega)$ at $\omega \to 0$, i.e. the value of κ_1 = 0.070, are useful in identifying the approach to a critical point of a system (Varotsos et al., 2011b), as that of seismicity (Varotsos et al., 2005b; Sarlis et al., 2008, 2009; Vallianatos

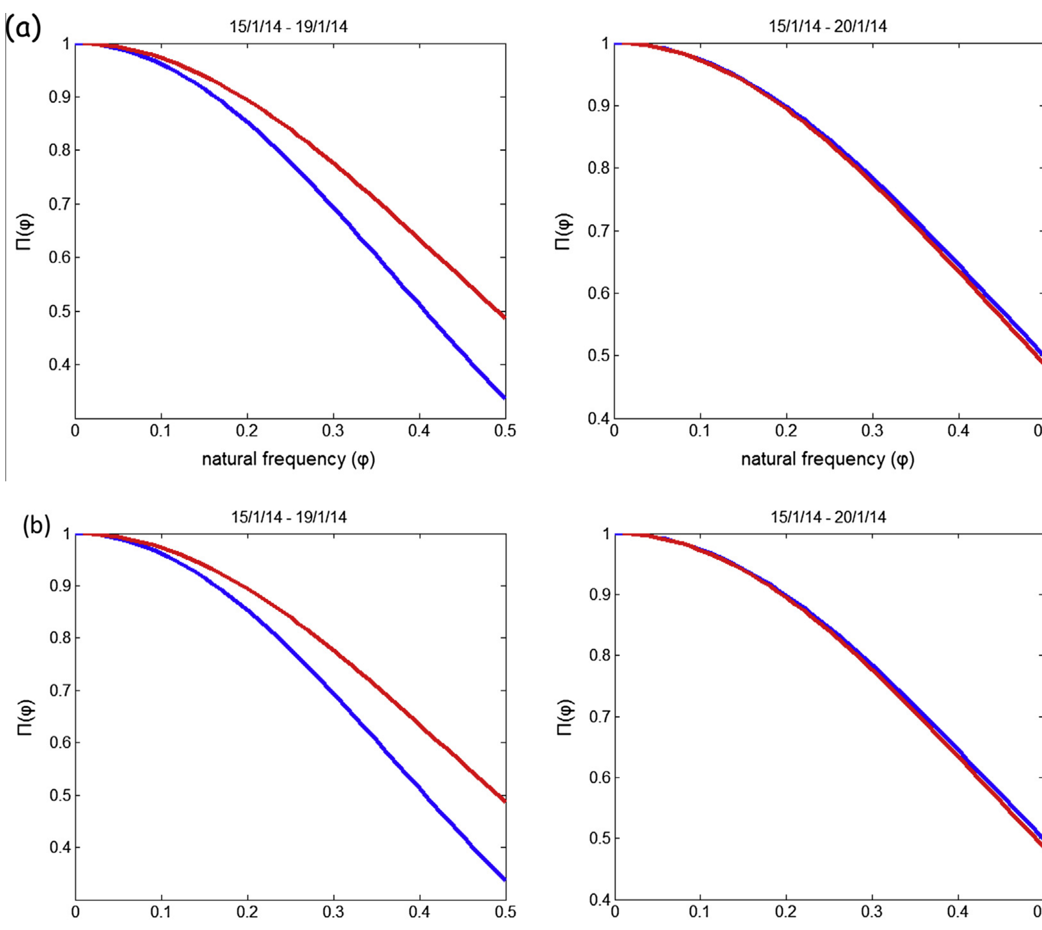

Fig. 8. Time evolution of $\Pi(\phi)$ for $0 \leqslant \phi \leqslant 0.5$ of the seismic activity for (a) $M_L \geqslant 2.0$ and R = 30 km, (b) $M_L \geqslant 2.0$ and R = 50 km, when the calculation was started on January 15, 2014. $\Pi(\phi)$ curves (blue) fall on the theoretical $\Pi(\phi)$ curve (red) calculated from Eq. (6) as critical stage is approached. (For interpretation of the references to colour in this figure legend, the reader is referred to the web version of this article.)

et al., 2014 and references therein). In Fig. 7c, the solid curve based on Eq. (6) represents critical stage with $\kappa_1 = 0.070$. The two other curves are referred to non critical stages. For instance, theoretically κ_1 was shown to approach 0.083 as $N \to \infty$ when there is no long-ranged correlation (Varotsos et al., 2011a), while the empirical κ_1 values for electric noises emitted from nearby artificial sources, were found to be significantly greater than 0.07 (see Varotsos et al., 2011a and references therein), indicating less than critical long-ranged correlation in these noises.

Note that κ_1 varies when a new event occurs, as (χ_k, p_k) are rescaled. It has been verified that this analysis allows for the detection of the entrance of system to the critical state by the convergence of the parameter κ_1 to the value 0.070 (Varotsos et al., 2008; Uyeda et al., 2009). Furthermore, the entropy in natural time, S_{nt}, is defined as (Varotsos et al., 2005a, 2006, 2011a):

$$S_{nt} = \langle \chi \ln \chi \rangle - \langle \chi \rangle \ln \langle \chi \rangle = \sum_{k=1}^{N} p_k \chi_k \ln \chi_\kappa - \left(\sum_{\kappa=1}^{N} p_k \chi_k \right) \ln \left(\sum_{\kappa=1}^{N} p_k \chi_k \right),$$

$$\text{where } \langle f(\chi) \rangle = \sum_{\kappa=1}^{N} p_k f(\chi_k).$$

The entropy in natural time is a dynamic quantity depending on the sequential order of events. The entropy, $S_{nt\_}$, obtained upon considering the time reversal T, i.e., $Tp_m = p_{N-m+1}$, is also studied, since a system is considered to approach criticality when the following conditions, are required for the analysed seismicity to correspond to a true critical state (Varotsos et al., 2008, 2011a, 2011b; Uyeda et al., 2009):

(i) The "average" distance D between the curves of normalized power spectra $\Pi(\omega)$ of the evolving seismicity and the theoretical estimation of $\Pi(\omega)$ for $\kappa_1 = 0.070$ should be smaller than 10^{-2}.
(ii) The parameter κ_1 should approach the value for $\kappa_1 = 0.070$ "by descending from above."
(iii) Both natural time entropies S_{nt} and $S_{nt\_}$ should be lower than the entropy of uniform noise $S_u = (\ln 2/2) - 1/4$ when κ_1 approaches the value $\kappa_1 = 0.070$.
(iv) Since the process concerned is expected to be self similar, in the critical state, the time of the true coincidence should not vary upon changing (*within reasonable limits*) either the magnitude threshold, M_{th}, or the area, used in the calculation.

Taking into account the MRWA result in lower scales we may propose the use of derived (in the frame of MRWA) time marker, which observed 12 days before major event, as an objective initiation point for the Natural Time analysis that will follow. The purpose for this proposal is to combine the two independent methods (MRWA and NT analysis) that have been successfully used for the identification of critical stages in earthquake preparation processes, in a joint approach that will maximize the advantages of each one. More specific, the initial application of MRWA in a broader time period, reveals time segment where the NT analysis is going to investigate, defining indicators suggesting the entrance to critical stage.

Fig. 8 clearly demonstrates that for a threshold magnitude of $M_{\text{th}} = 2.0$ and for two areas of radius $R = 30$ km and $R = 50$ km, respectively, around the epicenter of the main event, the computed $\Pi(\phi)$ curve approaches the critical $\Pi(\phi)$ curve, on January 20, 2014, a few days before the Mw6.1 earthquake of 26/1/2014. The approach of the two curves is more clearly demonstrated as the parameter D is plotted (Fig. 9). It may, thus, be considered that the critical point for seismicity was approached around that time. What happened during the whole study period and till January 26, 2014, can be seen in Fig. 9, which depicts D, κ_1, S_{nt}, and $S_{nt\_}$ as they evolved event by event.

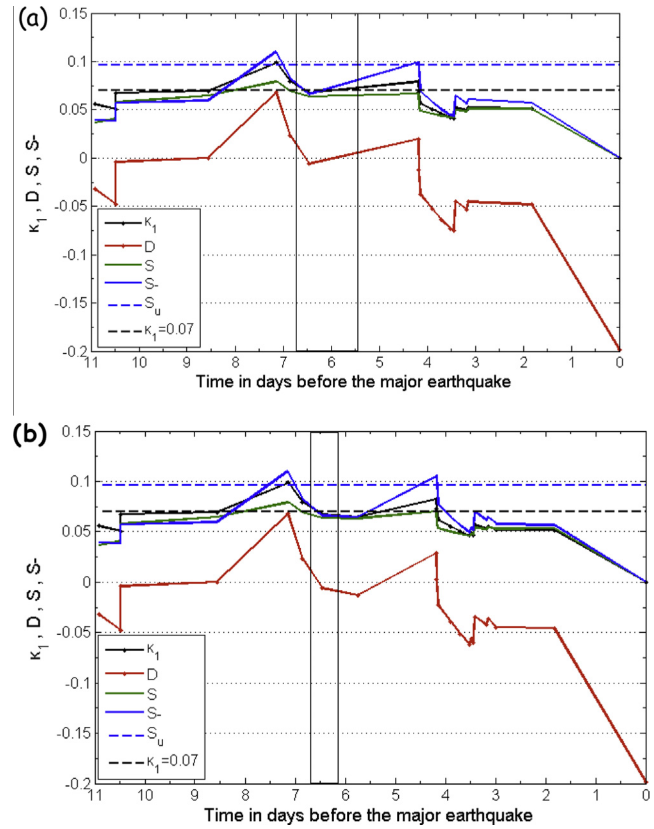

Fig. 9. Time evolution of the natural time analysis quantities κ_1; S_{nt}; $S_{nt\_}$, and D relative to new event occurrence prior to the Cephalonia Mw6.4 event, considering an area with radius of (a) $R = 30$ km and (b) $R = 50$ km, around the epicenter, for a magnitude thresholds, $M_{\text{th}} = 2.0$. The analysis starts on 15/1/2014. The up horizontal line indicates the entropy limit of $S_u = 0.0966$, while the value $\kappa_1 = 0.070$ noted on the scale. The rectangle marks the time when the critical stage is approached.

Starting from the time where the result of MRWA indicate a marker in lower scales (i.e., almost 12 days before major event) as the initiation point for the Natural Time analysis, natural time analysis applied to the seismicity occurred during the last weeks prior to the Mw6.1 event. We observe that all criticality requirements are fulfilled. Indeed, considering initially radius 30 km and 50 km around the epicenter, we observe that all the requirements are met at approximately January 20, 2014 (a few days before the main shock) for a magnitude threshold $M_{\text{th}} = 2.0$ (see Fig. 9). Thus, there is strong evidence that seismicity around the epicenter presents criticality characteristics a few days before the main event.

5. Conclusions

In the present work an analysis in the natural time domain has been carried out, using as a starting point that marked by the decreasing of the standard deviation of the wavelet coefficients $\sigma_{wav}(m)$, specially at lower scales, in a similar way as observed by Telesca et al. (2004, 2007) before a number of major earthquake events. We combine the two independent methods (MRWA and NT analysis) that have been successfully used for the identification of critical stages in earthquake preparation processes, in a joint approach that will maximize the advantages of each one. More specific, the initial application of MRWA in a broader region around the epicenter and for a time period long enough before the main event, reveals time segment where the NT analysis is going to investigate for indicators suggesting the entrance to critical stage.

We can state that the natural time analysis of the earthquake catalogue revealed that the order parameter κ_1 of the seismicity in the Cephalonia region shares a characteristic feature similar to that of non-equilibrium critical systems. Before the Mw6.1 earthquake on January 26, 2014, strong evidence of criticality in seismicity was observed within a few days before the main event. In other words, the curve of $\Pi(\phi)$ of seismicity in natural time domain coincided with the theoretical curve of critical phenomena shortly before this Mw6.1 event, for a M_{th} = 2.0 magnitude threshold. Thus, the analysis in the natural time domain of the seismicity initiated using the results of MRWA, led to estimation on the date of the impending large Mw6.1 earthquake of 26/01/2014, with a narrow time window of the order of a few days.

Acknowledgments

This work was supported by the THALES Program of the Ministry of Education of Greece and the European Union in the framework of the project entitled "Integrated understanding of Seismicity, using innovative Methodologies of Fracture mechanics along with Earthquake and non-extensive statistical physics – Application to the geodynamic system of the Hellenic Arc. SEISMO FEAR HELLARC".

References

Abe, S., Sarlis, N., Skordas, E., Tanaka, H., Varotsos, P., 2005. Origin of the usefulness of the natural-time representation of complex time series. Phys. Rev. Lett. 94, 170601. http://dx.doi.org/10.1103/PhysRevLett.94.170601.

Abe, S., Suzuki, N., 2005. Scale-free statistics of time interval between successive earthquakes. Phys. A: Stat. Mech. Appl. 350 (2–4), 588–596.

Abry, P., Flandrin, P., Taqqu, M.S., Veitch, D., 2000. Wavelets for the analysis, estimation, and synthesis of scaling data. In: Abry, P., Flandrin, P., Taqqu, M.S., Veitch, D. (Eds.), Self-Similar Network Traffic and Performance Evaluation. Wiley.

Abry, P., Flandrin, P., Taqqu, M.S., Veitch, D., 2002. Self-similarity and long-range dependence through the wavelet lens. In: Doukhan, P., Oppenheim, G., Taqqu, M.S. (Eds.), Theory and Applications of Long-Range Dependence. Birkhäuser, pp. 527–556.

Abry, P., Veitch, D., 1998. Wavelet analysis of long-range dependent traffic. IEEE Trans. Inform. Theory 44 (1), 2–15.

Antonopoulos, C.G., Michas, G., Vallianatos, F., Bountis, T., 2014. Evidence of q-exponential statistics in Greek seismicity. Phys. A: Stat. Mech. Appl. 409, 71–77.

Bak, P., Tang, C., 1989. Earthquakes as a self-organized critical phenomenon. J. Geophys. Res. 94 (15635-15), 637.

Corral, Á., Christensen, K., 2006. Comment on "earthquakes descaled: on waiting time distributions and scaling laws". Phys. Rev. Lett. 96 (10), 109801.

D'Alessandro, A., Papanastassiou, D., Baskoutas, I., 2011. Hellenic Unified Seismological Network: an evaluation of its performance through SNES method. Geophys. J. Int. 185, 1417–1430.

Davidsen, J., Goltz, C., 2004. Are seismic waiting time distributions universal? Geophys. Res. Lett. 31 (21), L21612 1-4.

Godano, C., Caruso, V., 1995. Multifractal analysis of earthquake catalogues. Geophys. J. Int. 121, 385–392.

Ganas, A., Cannavò, F., González, P.J., Drakatos, G., 2014. The Geodetic Signature of the January 26, 2014 Earthquake Onshore Cephalonia, Greece, Unpublished Report. <http://www.gein.noa.gr/Documents/pdf/VLSM_co-seismic_26-1-2014_13_55_UTC.pdf>.

Hainzl, S., Scherbaum, F., Beauval, C., 2006. Estimating background activity based on interevent-time distribution. Bull. Seismol. Soc. Am. 96, 313–320.

Hollenstein, C., Müller, M.D., Geiger, A., Kahle, H.G., 2008. Crustal motion and deformation in Greece from a decade of GPS measurements, 1993–2003. Tectonophysics 449 (1–4), 17–40.

Karakostas, V., Papadimitriou, E., Mesimeri, M., Gkarlaouni, C., Paradisopoulou, P., 2014. The 2014 Kefalonia doublet (Mw6.1 and Mw6.0), Central Ionian Islands, Greece: seismotectonic implications along the Kefalonia transform fault zone. Acta Geophys. http://dx.doi.org/10.2478/s11600-014-0227-4.

Karastathis, V., Koukouvelas, I., Ganas, A., Moschou, A., Mouzakiotis, A., Papadopoulos, G.A., Spanos, D., 2014. The strong M_w6 earthquake of 26th January 2014 in Cephalonia Island, Ionian Sea, Greece: a first report. Geophys. Res. Abstr. 16, EGU2014-17001.

Kiratzi, A., Langston, C., 1991. Moment tensor inversion of the January 17, 1983 Kefallinia event of Ionian Islands. Geophys. J. Int. 105, 529–535.

Kokinou, E., Papadimitriou, E., Karakostas, V., Kamberis, V., Vallianatos, F., 2006. The Kefalonia Transform Zone (offshore Western Greece) with special emphasis to its prolongation towards the Ionian Abyssal Plain. Mar. Geophys. Res. 27, 241–252. http://dx.doi.org/10.1007/s11001-006-9005-2.

Kiyashchenko, D., Smirnova, N., Troyan, V., Vallianatos, F., 2003. Dynamics of multifractal and correlation characteristics of the spatio-temporal distribution of regional seismicity before the strong earthquakes. Nat. Hazards Earth Syst. Sci. 3, 285–298.

Kiyashchenko, D., Smirnova, N., Troyan, V., Vallianatos, F., 2004. Seismic hazard precursory evolution: fractal and multifractal aspects. Phys. Chem. Earth 29, 367–378.

Lapenna, V., Macchiato, M., Piscitelli, S., Telesca, L., 2000. Scale-invariance properties in seismicity of Southern Apennine Chain (Italy). Pure Appl. Geophys. 157 (4), 589–601.

Lekkas, E., Danamos, G., Mavrikas, G., 2001. Geological structure and evolution of Cephalonia and Ithaki Islands. Bull. Geol. Soc. Greece XXXIV/1, 11–17.

LePichon, X., Lallement, S.J., Chamont-Rooke, N., Lemeur, D., Pascal, G., 2002. The Mediterranean Ridge backstop and the Hellenic nappes. Mar. Geol. 186, 111–125.

Louvari, E., Kiratzi, A., Papazachos, B.C., 1999. The Cephalonia Transform Fault and its extension to western Lefkada island (Greece). Tectonophysics 308, 223–236.

Michas, G., Vallianatos, F., Sammonds, P., 2013. Non-extensivity and long-range correlations in the earthquake activity at the West Corinth rift (Greece). Nonlinear Process. Geophys. 20, 713–724.

Mignan, A., Chouliaras, G., 2014. Fifty years of seismic network performance in Greece (1964–2013): spatiotemporal evolution of the completeness magnitude. Seismol. Res. Lett. 85, 657–667.

Öncel, A.O., Main, I.G., Alptekin, O., Cowie, P.A., 1996. Spatial variation in the fractal properties of seismicity in the north Anatolian fault zone. Tectonophysics 257, 189–202.

Papadakis, G., Vallianatos, F., Sammonds, P., 2013. Evidence of nonextensive statistical physics behavior of the Hellenic subduction zone seismicity. Tectonophysics 608, 1037–1048.

Papadimitriou, E., 2002. Document mode of strong earthquake recurrence in the central Ionian Islands (Greece): possible triggering due to Coulomb stress changes generated by the occurrence of previous strong shocks. Bull. Seismol. Soc. Am. 92 (8), 3293–3308.

Papadimitriou, E., Papazachos, B.C., 1985. Seismicity gaps in the Aegean and surrounding area. B. Geofis. Teorica Appl. 27 (107), 185–195.

Papanastassiou, D., 2010. Earthquake detection–location capability of the Hellenic Unified Seismological Network (HUSN) operating by the Institute of Geodynamics, National Observatory of Athens. Hellenic J. Geosci. 45, 109–216.

Papazachos, B.C., Papazachou, C.B., 1997. The Earthquakes of Greece. Ziti Publ, Thessaloniki, Greece, 304pp.

Papazachos, C.B., Kiratzi, A., 1996. A detailed study of the active crustal deformation in the Aegean and surrounding area. Tectonophysics 253 (1–2), 129–153.

Rundle, J.B., Turcotte, D.L., Shcherbakov, R., Klein, W., Sammis, C., 2003. Statistical physics approach to understanding the multiscale dynamics of earthquake fault systems. Rev. Geophys. 41 (4), 5-1-5.30.

Sachpazi, M., Hirn, A., Clement, C., Haslinger, F., Laigle, M., Kissling, E., Charvis, P., Hello, Y., Lepine, J.C., Sapin, M., Ansorge, J., 2000. Western Hellenic subduction and Cephalonia Transform: local earthquakes and plate transport and strain. Tectonophysics 319, 301–319.

Sarlis, N.V., Skordas, E.S., Lazaridou, M.S., Varotsos, P.A., 2008. Investigation of seismicity after the initiation of a seismic electric signal activity until the main shock. Proc. Jpn. Acad. Ser. B 84, 331–343.

Sarlis, N.V., Skordas, E.S., Varotsos, P.A., 2009. Multiplicative cascades and seismicity in natural time. Phys. Rev. E – Stat., Nonlinear, Soft Matter Phys. 80 (2), 022102.

Sarlis, N.V., Skordas, E.S., Varotsos, P.A., 2010. Nonextensivity and natural time: the case of seismicity. Phys. Rev. E 82, 021110.

Scordilis, E., Karakaisis, G., Karakostas, V., Panagiotopoulos, D., Comninakis, P., Papazachos, B.C., 1985. Evidence for transform faulting in the Ionian Sea: the Cephalonia Island earthquake sequence of 1983. Pure Appl. Geophys. 123, 388–397.

Sornette, D., 2000. Critical Phenomena in Natural Sciences. Springer, Berlin, EU.

Teich, M.C., Heneghan, C., Lowen, S.B., Turcott, R.G., 1996. Estimating the fractal exponent of point processes in biological systems using wavelet- and Fourier-transform methods. In: Aldroubi, A., Unser, M. (Eds.), Wavelets in Medicine and Biology. CRC Press, Boca Raton, FL, pp. 383–412.

Telesca, L., Cuomo, V., Lapenna, V., Vallianatos, F., 2000. Self-similarity properties of seismicity in the Southern Aegean area. Tectonophysics 321 (1), 179–188.

Telesca, L., Cuomo, V., Lapenna, V., Macchiato, M., 2001. Statistical analysis of fractal properties of point processes modeling seismic sequences. Phys. Earth Planet. Int. 125, 65–83.

Telesca, L., Lapenna, V., Vallianatos, F., 2002. Monofractal and multifractal approaches in investigating scaling properties in temporal patterns of the 1983–2000 seismicity in the western Corinth graben, Greece. Phys. Earth Planet. Int. 131, 63–79.

Telesca, L., Lapenna, V., Alexis, N., 2004. Multiresolution wavelet analysis of earthquakes. Chaos Soliton Fract. 22, 741–748.

Telesca, L., Macchiato, M., 2004. Time-scaling properties of the Umbria–Marche 1997–1998 seismic crisis, investigated by the detrended fluctuation analysis of interevent time series Chaos. Solitons Fractals 19 (2), 377–385.

Telesca, L., Hloupis, G., Nikolintaga, I., Vallianatos, F., 2007. Temporal patterns in southern Aegean seismicity revealed by the multiresolution wavelet analysis. Commun. Nonlinear Sci. Numer. Simul. 12 (8), 1418–1426.

Thurner, S., Lowen, S.B., Feurstein, M.C., Heneghan, C., Feichtinger, H.G., Teich, M.C., 1997. Analysis, synthesis, and estimation of fractal-rate stochastic point processes. Fractals 5, 565–596.

Tsallis, C., 2009. Introduction to Nonextensive Statistical Mechanics: Approaching a Complex World. Springer, Berlin.
Tzanis, A., Vallianatos, F., Makropoulos, K., 2000. Seismic and electrical precursors to the 17-1-1983, M7 Kefallinia earthquake, Greece: signatures of a SOC system. Phys. Chem. Earth, Part A: Solid Earth Geodesy 25 (3), 281–287.
Uritsky, V., Smirnova, N., Troyan, V., Vallianatos, F., 2004. Critical dynamics of fractal fault systems and its role in the generation of pre-seismic electromagnetic emissions. Phys. Chem. Earth 29, 473–480.
Uyeda, S., Kamogawa, M., Tanaka, H.K., 2009. Analysis of electrical activity and seismicity in the natural time domain for the volcanic-seismic swarm activity in 2000 in the Izu Island region, Japan. J. Geophys. Res. 114, B02310.
Valkaniotis, S., Ganas, A., Papathanassiou, G., Papanikolaou, M., 2014. Field observations of geological effects triggered by the January–February 2014 Cephalonia (Ionian Sea, Greece) earthquakes. Tectonophysics 630 (1), 150–157.
Vallianatos, F., Michas, G., Benson, P., Sammonds, P., 2013. Natural time analysis of critical phenomena: the case of acoustic emissions in triaxially deformed Etna basalt. Phys. A: Stat. Mech. Appl. 392 (20), 5172–5178.
Vallianatos, F., Michas, G., Papadakis, G., 2014. Non-extensive and natural time analysis of seismicity before the Mw6.4, October 12, 2013 earthquake in the South West segment of the Hellenic Arc. Phys. A: Stat. Mech. Appl. 414, 163–173.
Varotsos, P.A., Sarlis, N.V., Skordas, E.S., 2002. Long-range correlations in the electric signals that precede rupture. Phys. Rev. E 66 (1), 011902/1–011902/7.
Varotsos, P.A., Sarlis, N.V., Skordas, E.S., Lazaridou, M., 2005a. Natural entropy fluctuations discriminate similar-looking electric signals emitted from systems of different dynamics. Phys. Rev. E 71, 011110. http://dx.doi.org/10.1103/PhysRevE.71.011110.
Varotsos, P.A., Sarlis, N.V., Tanaka, H.K., Skordas, 2005b. Similarity of fluctuations in correlated systems: the case of seismicity. Phys. Rev. E 72, 041103. http://dx.doi.org/10.1103/PhysRevE.72.041103.
Varotsos, P.A., Sarlis, N.V., Skordas, E.S., Tanaka, H.K., Lazaridou, M., 2006. Entropy of seismic electric signals: analysis in natural time under time reversal. Phys. Rev. E 74, 021123.
Varotsos, P.A., Sarlis, N.V., Skordas, E.S., Lazaridou, M.S., 2008. Fluctuations, under time reversal, of the natural time and the entropy distinguish similar looking electric signals of different dynamics. J. Appl. Phys. 103, 014906.
Varotsos, P.A., Sarlis, N.V., Skordas, E.S., 2009. Detrended fluctuation analysis of the magnetic and electric field variations that precede rupture. CHAOS 19, 023114.
Varotsos, P.A., Sarlis, N.V., Skordas, E.S., 2011a. Natural Time Analysis: The New View of Time. Precursory Seismic Electric Signals, Earthquakes and Other Complex Time-Series. Springer-Verlag, Berlin, Heidelberg.
Varotsos, P., Sarlis, N.V., Skordas, E.S., Uyeda, S., Kamogawa, M., 2011b. Natural time analysis of critical phenomena. Proc. Natl. Acad. Sci. USA 108, 11361–11364.
Wornell, G., 1995. Signal Processing with Fractals: A Wavelet based Approach. Prentice-Hall.
Zoeller, G., Hainzl, S., 2002. A systematic spatiotemporal test of the critical point hypothesis for large earthquakes. Geophys. Res. Lett. 29, 53-1-4.